

Supporting Information

An ultra-stable bio-inspired bacteriochlorin analogue for hypoxic-tolerance photodynamic therapy

Mengsi Wu⁺, Zhiyong Liu⁺ and Weian Zhang^{*}

Shanghai Key Laboratory of Functional Materials Chemistry, East China University of Science and Technology, 130
Meilong Road, Shanghai 200237, China

MATERIALS AND METHODS

Materials

Dichloromethane (DCM) and *N, N*-dimethylformamide (DMF) were dried over with calcium hydride (CaH₂) and distilled before use. *p*-Toluenesulfonyl hydrazide (TSH) was purchased from J&K Scientific Ltd (Shanghai, China). SH-PEG-SH (2000 Da) was purchased from Shanghai ToYongBio Tech. Inc. Singlet oxygen sensor green (SOSG), dihydroethidium (DHE), 3'-(4-hydroxyphenyl) fluorescein (HPF), Fetal bovine serum (FBS), Dulbecco's modified Eagle's medium (DMEM), Hoechst 33342 and 3-(4,5-dimethylthiazol-2-yl)-2,5-diphenyltetrazolium bromide (MTT) were purchased from Shanghai Maokang Biotechnology Co.,Ltd.

Measurements

¹H NMR and ¹⁹F NMR spectra in CDCl₃ were obtained on a Bruker AVANCE III HD 400 Spectrometer. The UV-vis absorption spectra of the samples were measured by a Thermo Scientific Evolution 220 spectrophotometer over different irradiation time intervals. Dynamic light scattering (DLS) was performed on a Litesizer particle analyzer at room temperature. Transmission electron microscopy (TEM) was observed on a JEOL JEM1400 electron microscope operated at 100 kV. Fluorescence quantum yield was measured by HAMAMATSU Quantaurus-QY C11347-11.

Methods

Synthesis of FBC

TFPP was synthesized according to the previous works¹⁻². **TFPP** (250 mg, 0.26 mmol) and 1.45 g (7.8 mmol) of *p*-toluenesulfonyl hydrazide (TSH) were placed in a mortar, and then grinded evenly. The powder was put into a Schlenk flask and kept under vacuum for 2 h. Subsequently, the mixture was heated to 158 °C for 18 min. After cooling to room temperature, the mixture purified by silica gel chromatograph to obtain the product **FBC**.

Synthesis of FBC-80 nanogels

FBC (10 mg, 0.03 mmol) and SH-PEG-SH (122 mg, 0.06 mmol, $M_n = 2000 \text{ g mol}^{-1}$) were dissolved in 10 mL of *N, N*-dimethylformamide (DMF) under a nitrogen atmosphere. Then, diethylamine (12 μL) was added into the solution and the mixture was stirred at room temperature for 8 h. Then, the solution was transferred to a dialysis bag (MWCO = 3500) and dialyzed for 72 h against ultrapure water. Finally, the product of **FBC-80** was obtained by freeze-drying.

Synthesis of FBC-200 nanogels

FBC-200 was synthesized in a similar way with that of **FBC-80**, in which the volume of DMF was only changed into 1 mL.

Reactive oxygen species (ROS) detection

ROS generation was determined by using a ROS capture agent 1,3-diphenylisobenzofuran (DPBF), which could capture and react with ROS rapidly. A mixed solution containing **FBC** and DPBF was added into a quartz cuvette and irradiated at 750 nm. The ROS generation of **FBC** can be directly correlated with the decrease of the DPBF absorbance in the UV-vis spectrum, thus the absorbance of DPBF was measured every 10 s.

Singlet Oxygen ($^1\text{O}_2$) detection

Singlet oxygen ($^1\text{O}_2$) generation was confirmed by the increase of emission at 530 nm of singlet oxygen sensor green (SOSG). 20 μL SOSG solution (1 mM) was added into the solution of 2 mL **FBC** or **FBC** nanogels. The solution containing SOSG with **FBC** or **FBC** nanogels was irradiated by 750 nm, and the fluorescence changes were detected every 10 s with the excitation wavelength of 490 nm.

Singlet Oxygen quantum yield

Singlet oxygen quantum yields (Φ_Δ) of the porphyrin units in copolymers were measured in accordance with the previous literature³. The Φ_Δ was determined using 9,10-Anthracenediyl-bis(methylene)-dimalonic acid (ABDA) as a scavenger of singlet oxygen and taking tetraphenyl porphyrin (TPP) as a standard. ABDA's decay at 360 nm was monitored at a certain interval. The value of Φ_Δ was calculated via the following equation:

$$\Phi_\Delta = \Phi_{\Delta\text{TPP}} \frac{S}{S_{\text{TPP}}}$$

where $\Phi_{\Delta\text{TPP}}$ is the singlet oxygen quantum yield of the standard TPP (0.62); S and S_{TPP} are ABDA's photobleaching rate in the presence of the samples and the standard TPP, respectively.

Superoxide anion radical ($\text{O}_2^{\cdot-}$) detection

Dihydroethidium (DHE) can be dehydrogenated to form ethidium by $\text{O}_2^{\cdot-}$, and ethidium can produce red fluorescence at 610 nm. The $\text{O}_2^{\cdot-}$ generation of can be directly correlated with the increase of the ethidium emission in the fluorescence spectrum. 20 μL DHE solution (10 mM) was added in to the solution of 2 mL samples. The fluorescence changes were detected after illumination with 750 nm laser, and the excitation wavelength was 490 nm.

Hydroxyl radical ($\cdot\text{OH}$) detection

Hydroxyl radical ($\cdot\text{OH}$) was detected by fluorescence spectroscopy using hydroxyphenyl fluorescein (HPF), which reacts with $\cdot\text{OH}$ to produce high fluorescence emission at 530 nm. HPF was dissolved in DMF to gain 5 mM HPF solution. Then, 20 μL HPF was added into the solution of 2 mL **FBC** or **FBC** nanogels. The fluorescence changes were detected after illumination with 750 nm laser, and the excitation wavelength was 490 nm.

Penetration ability evaluation

The penetration abilities of **FPC**, **PBC** and **FBC** were confirmed by the UV-vis spectroscopy of DPBF under the laser (50 mW/cm²) of 660 nm, 730 nm and 750 nm, respectively. Different thickness of pork skin (0.5 cm, 1.0 cm) was selected as barriers. The solution containing the photosensitizer and DPBF with or without barrier was irradiated by its corresponding laser, and the absorbance of DPBF was measured at regular intervals. The ratio of the degradation rate of DPBF with barrier to the degradation rate of DPBF without barrier has been calculated to reveal its penetrability.

Stability evaluation

The stability of photosensitizers was evaluated by UV-vis spectroscopy in the presentation of light (50 mW/cm²). The UV-vis absorbance spectra of **FPC**, **PBC** and **FBC** were measured every 1 min. In addition, **FBC** solution was placed at room temperature under visible light.

Cell Culture

4T1 murine breast cancer cells were cultivated in Dulbecco's modified Eagle's medium (DMEM) supplemented with 1% antibiotics (penicillin and streptomycin) and 10% fetal bovine serum (FBS) in a humidified standard atmosphere of 5% CO₂ at 37 °C.

Cellular Uptake Evaluation

The cellular uptake was observed by confocal laser scanning microscopy (CLSM). First, 4T1 cells (2 × 10⁴ cells/well) were seeded on glass bottom cell culture dishes for 24 h, and then the cells were treated with fresh medium containing **FBC**, **FBC-200** or **FBC-80** at the same concentration 50 µg/mL of porphyrin for 24 h, respectively. Next, cells were washed carefully and treated with 4% paraformaldehyde. Then, the cells nuclei were stained with Hoechst for 3 min and washed three times with PBS. Finally, the intracellular fluorescence of porphyrin was observed by CLSM with excitation at 510 nm and emission at 760 nm.

Intracellular ROS Generation Assay

The intracellular ROS generation was measured by using SOSG, HPF and DHE as probes. SOSG could be oxidized by ¹O₂ and then emits green fluorescence; HPF as a probe of •OH can react specifically with •OH to produce strong green fluorescence, and DHE can be dehydrogenated to form ethidium with red fluorescence by O₂^{•-}. Classically, 4T1 cells with DMEM media were incubated in glass bottom cell culture dishes for 24 h. Then, the 4T1 cells were incubated with **FBC** nanogels (50 µg/ml) with or without light irradiated (750 nm, 10 min, 100 mW·cm⁻²). Then, PBS containing SOSG (10 µM), HPF (10 µM) and DHE (12 µM) solution replaced the cells medium. After incubation for 30 min, the cells were observed *via* CLSM to confirm the ¹O₂, •OH or O₂^{•-} generation. The excitation wavelength was 488 nm.

In Vitro Cytotoxicity Assay

The cytotoxicity of **FBC** nanogels was evaluated by a standard MTT assay. 200 µL of 4T1 cell suspension (5 × 10³ cells/mL) was seeded in a 96-well plate and then incubated for 24 h at 37 °C. Different concentrations of **FBC**, **FBC-200** and **FBC-80** (porphyrin concentration at 0-16 µg/mL) in fresh DMEM

media were added into the wells and co-cultured for another 24 h, respectively. The cells were washed and irradiated with 750 nm laser (100 mW/cm²) for 15 min. Then, the cells were incubated for further 24 h. After that, the media was replaced with 200 μL of MTT solution (0.5 mg/mL in DMEM) and cultured for 4 h. Finally, 150 μL of DMSO per well was added to replace the MTT solution, and the absorbance value was recorded with a SpectraMax spectrometer at the wavelength of 492 nm. The *in vitro* dark cytotoxicity of **FBC** nanogels was assessed using the same procedure described above but without light illumination.

Animals and Tumor Xenograft Model

Tumor-bearing BALB/c mice were established and used for *in vivo* imaging: 4T1 cells (1 × 10⁶ cells in 200 μL of PBS) were subcutaneously injected into the mice, respectively. Once the volumes of tumor reached 100 mm³, the tumor-bearing mice were used for imaging or therapy. The tumor volume (V) was measured by the length and width of tumors and calculated as $V = 0.52 \times (\text{tumor length}) \times (\text{tumor width})^2$. Relative tumor volume was defined as V/V_0 (V_0 was the tumor volume when the treatment was initiated). All animal studies were conducted on male Balb/c nude mice (four to 5 weeks) in compliance with the National Institutes of Health Guide for the Care and Use of Laboratory Animals approved by the Animal Care and Use Committee of East China University of Science and Technology.

In Vivo Fluorescence Imaging

For fluorescence imaging, 200 μL of **FBC-200** or **FBC-80** (1 mg/mL porphyrin) was injected into tumor bearing mice through the tail vein. All the image acquisitions were performed with *in vivo* multispectral imaging system (Kodak FX) equipped with excitation band pass filter at 510 nm and emission at 770 nm when the mice were anesthetized at 0.5 h, 4 h, 10 h and 24 h post injection.

In Vivo Therapeutic Evaluation

The 4T1 tumor-bearing mice were chosen for therapeutic evaluation of **FBC** nanogels. After the tumor volume of the 4T1 tumor-bearing mice reached about 100 mm³, the mice were injected with different photosensitizers and divided into five groups (n = 4 for each group): (1) **PBS**, (2) **FBC-200**, (3) **FBC-80**, (4) **FBC-200+L** and (5) **FBC-80+L** (porphyrin concentration at 1 mg/kg). The power density of 750 nm laser was 200 mW/cm². The tumor volume was measured and calculated by vernier caliper every three days. The body weight of mice was also recorded during the experiment. Then, the mice were sacrificed on the 15th day. The tumors were dissected and weighed. The tumor inhibiting rates were calculated to evaluate the therapeutic efficacy. The dissected tumors were embedded in paraffin and made as 4 μm slices by cryosection. Furthermore, the frozen slices were stained with H&E to further characterize the therapeutic effects. The slices were imaged under an inverted fluorescence microscope.

Statistical analysis

Statistical analysis was performed by Student's t-test for two groups. All results were expressed as the mean ± s.d. unless otherwise noted. A value of $P < 0.05$ was considered statistically significant.

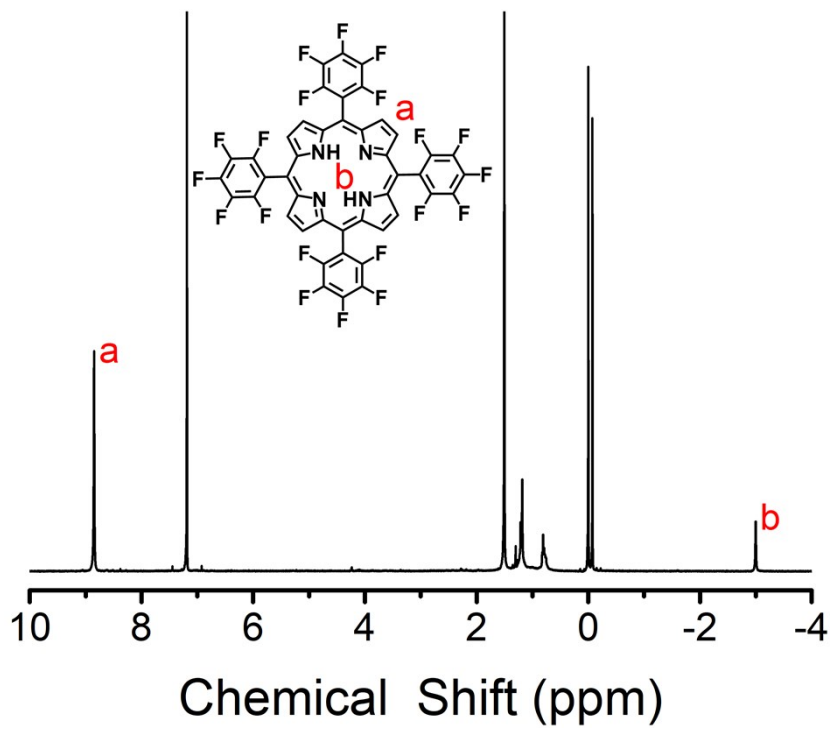


Fig. S1 ¹H NMR spectrum of TFPP.

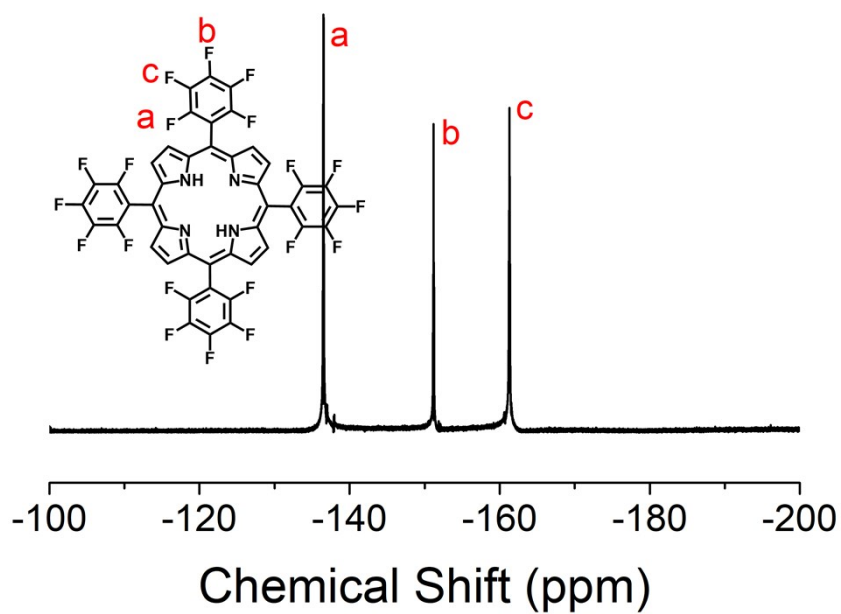


Fig. S2 ¹⁹F NMR spectrum of TFPP.

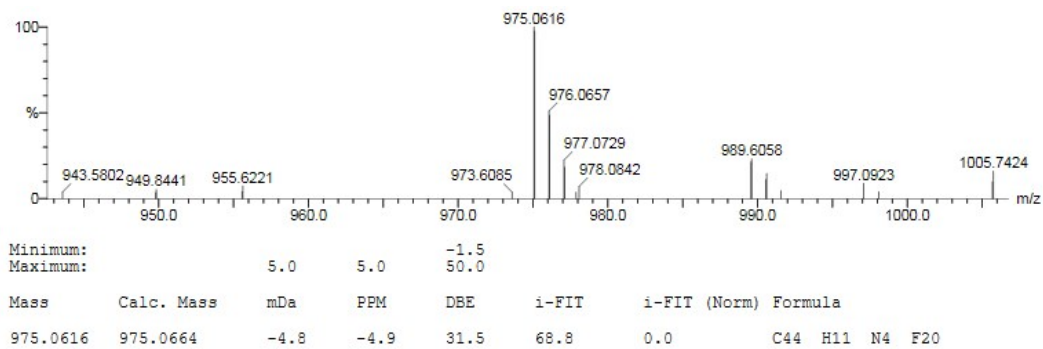


Fig. S3 MS spectrum of **TFPP**.

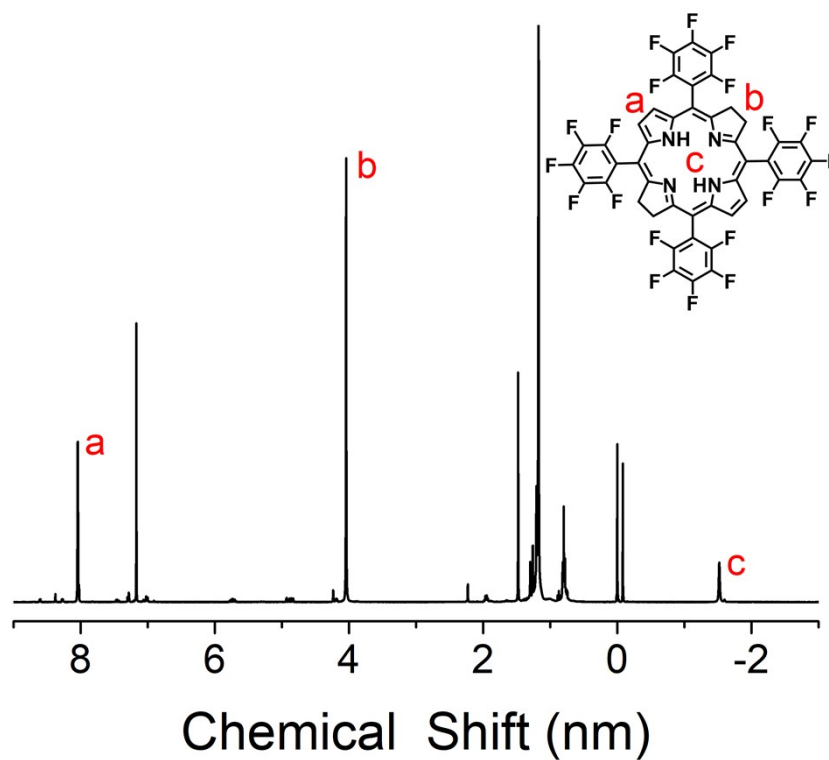


Fig. S4 ^1H NMR spectrum of **FBC**.

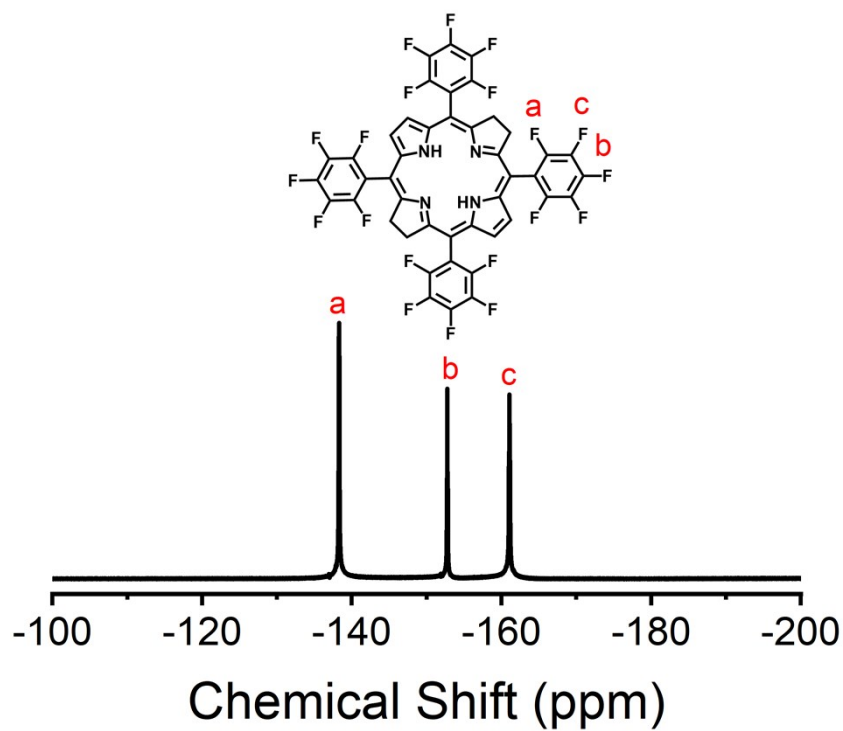


Fig. S5 ^{19}F NMR spectrum of **FBC**.

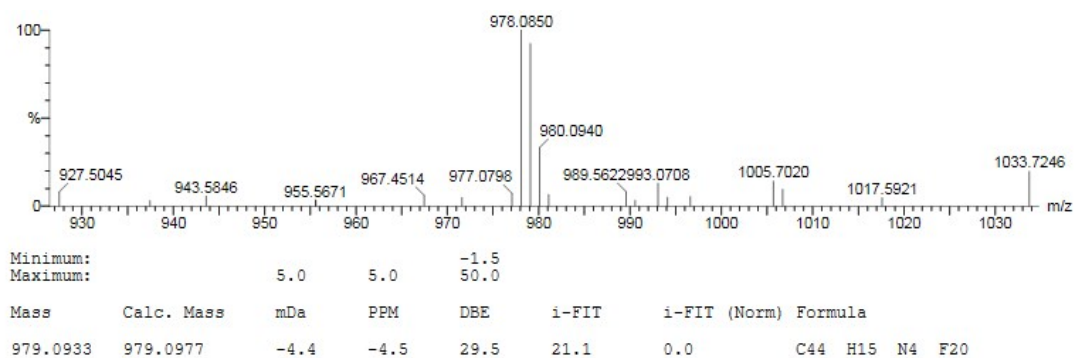


Fig. S6 MS spectrum of **FBC**.

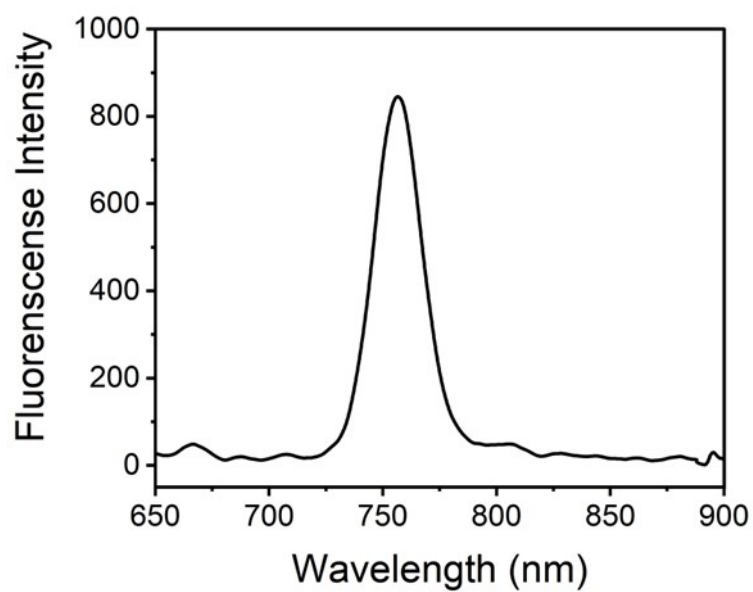


Fig. S7 Fluorescence emission spectrum of **FBC**.

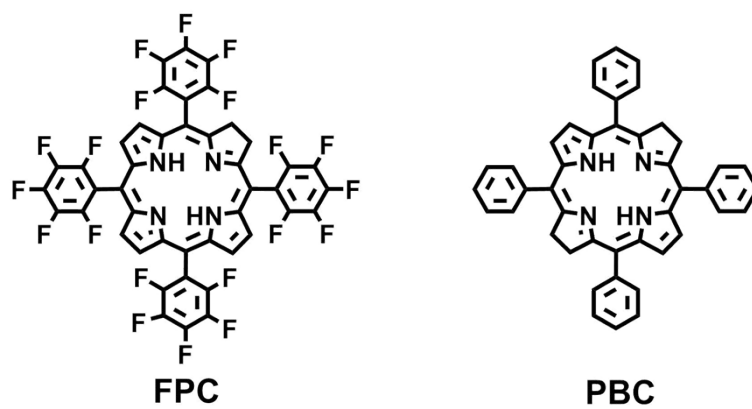


Fig. S8 Structures of **FPC** and **PBC**.

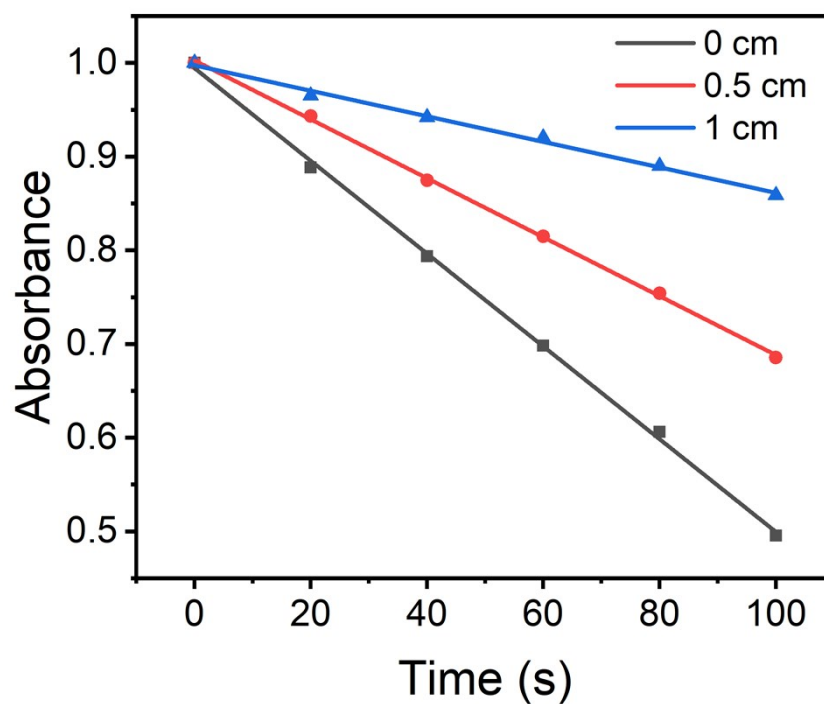


Fig. S9 The changes of ROS generation determined by DPBF with different thickness of pork skin under 660 nm laser.

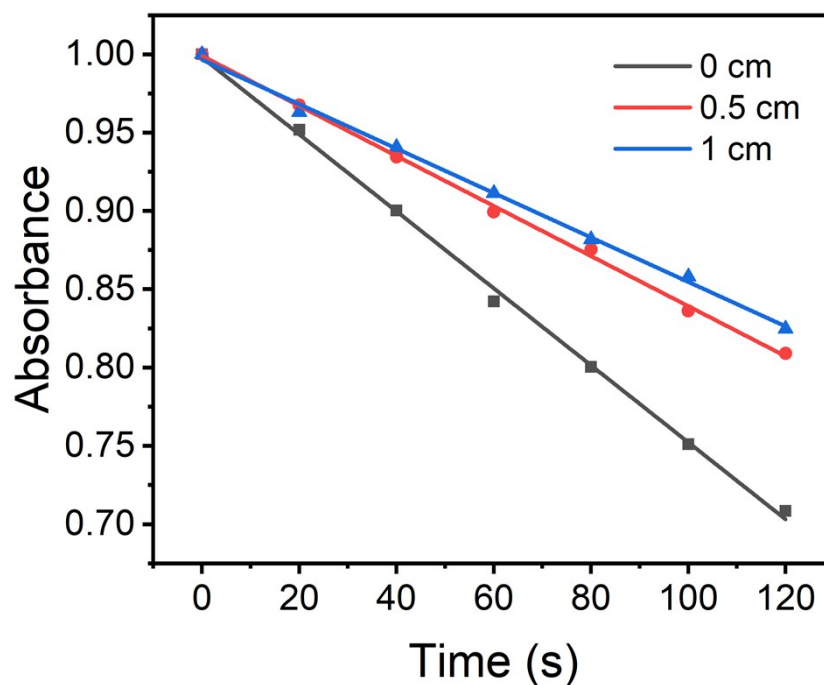


Fig. S10 The changes of ROS generation determined by DPBF with different thickness of pork skin under 730 nm laser.

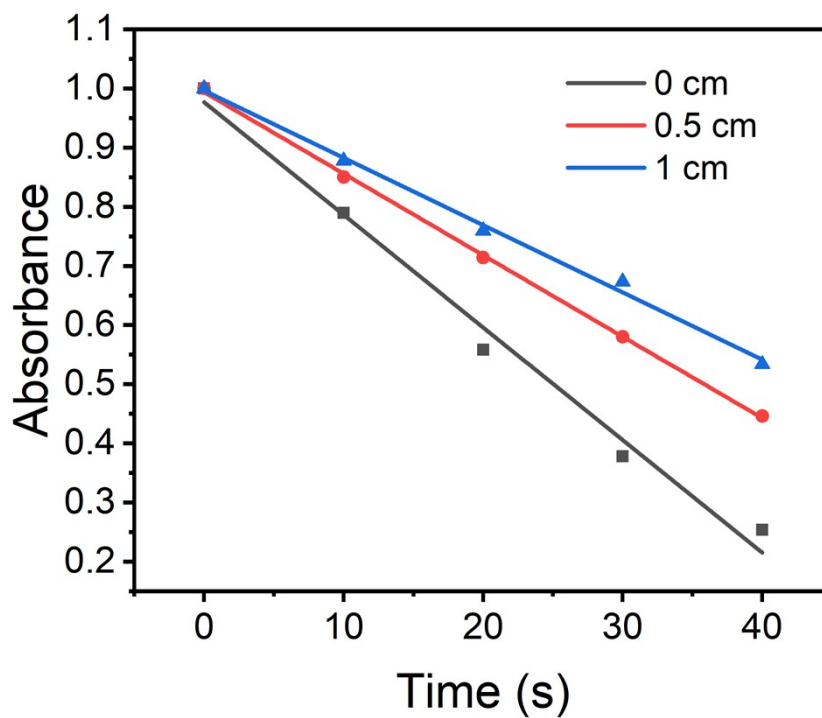


Fig. S11 The changes of ROS generation determined by DPBF with different thickness of pork skin under 750 nm laser.

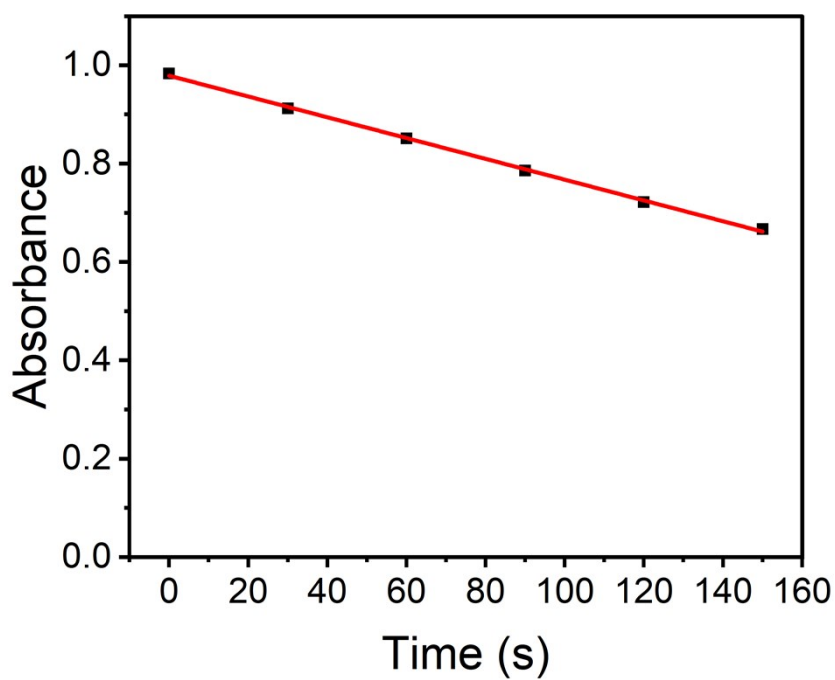


Fig. S12 The absorbance change of ABDA (at 360 nm) along with laser irradiation (750 nm laser at 50 mW·cm⁻²) in the presence of FBC.

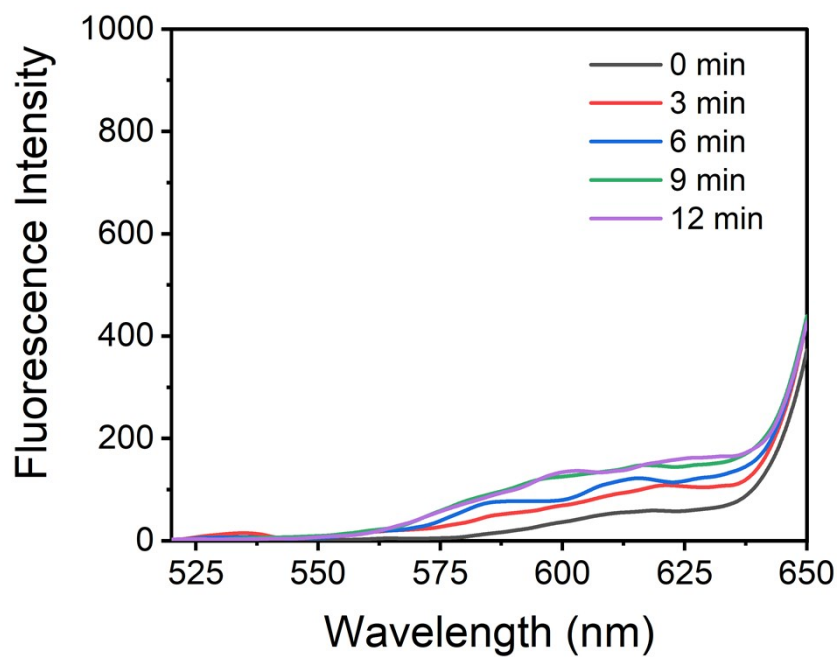


Fig. S13 Fluorescence spectrum of DHE for O_2^- detection of **FPC** with increasing illumination time.

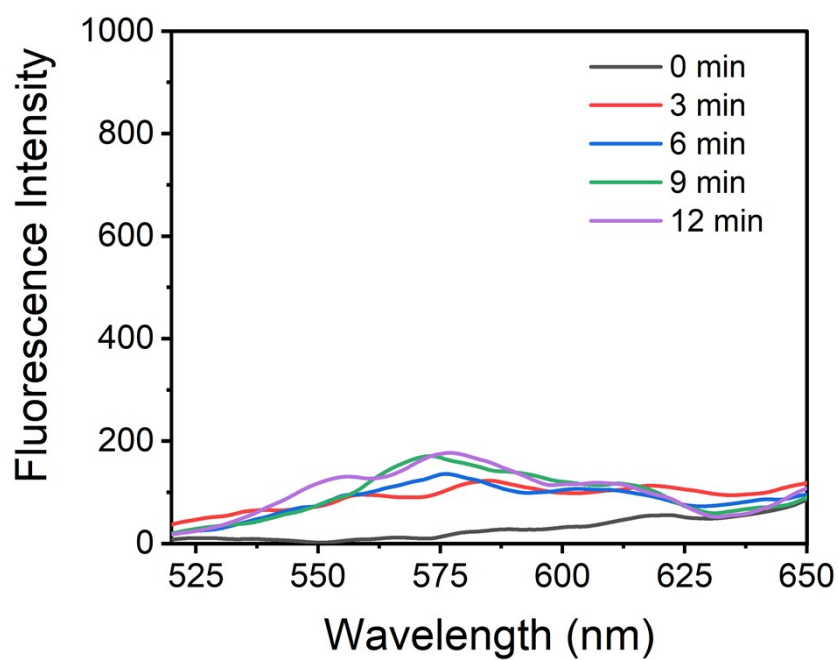


Fig. S14 Fluorescence spectrum of DHE for O_2^- detection of **PBC** with increasing illumination time.

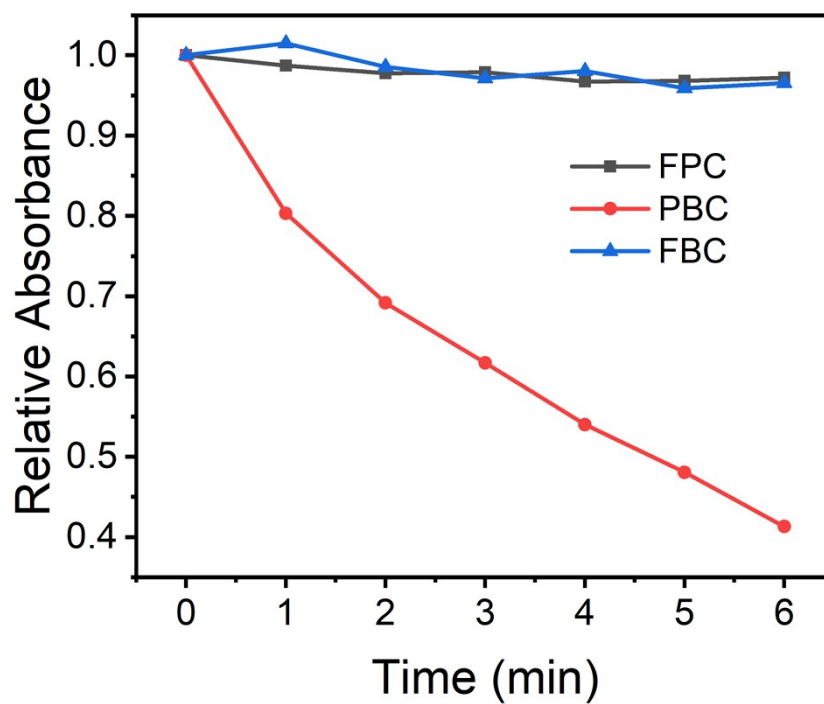


Fig. S15 Photostability of **FPC**, **PBC** and **FBC** with increasing illumination time.

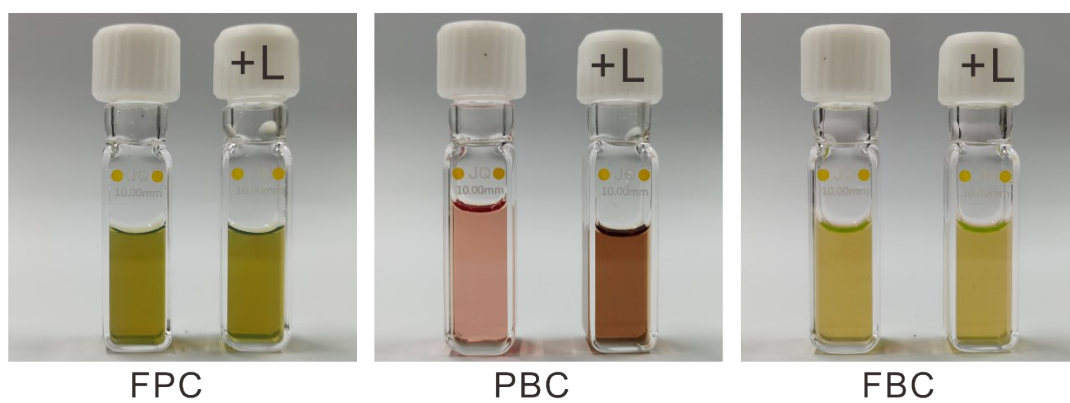


Fig. S16 Photographs of **FPC**, **PBC** and **FBC** before or after laser treatment.

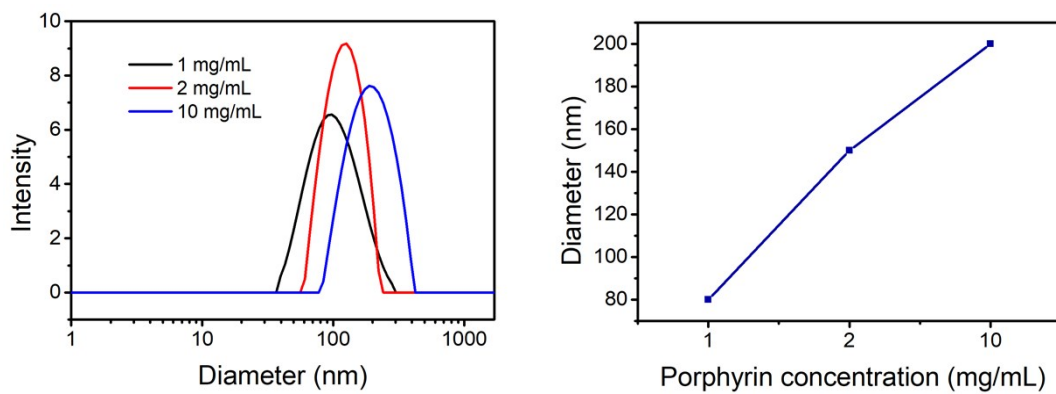


Fig. S17 DLS of **FBC** synthesized from reactants with different concentrations (left: size distribution; right: diameter).

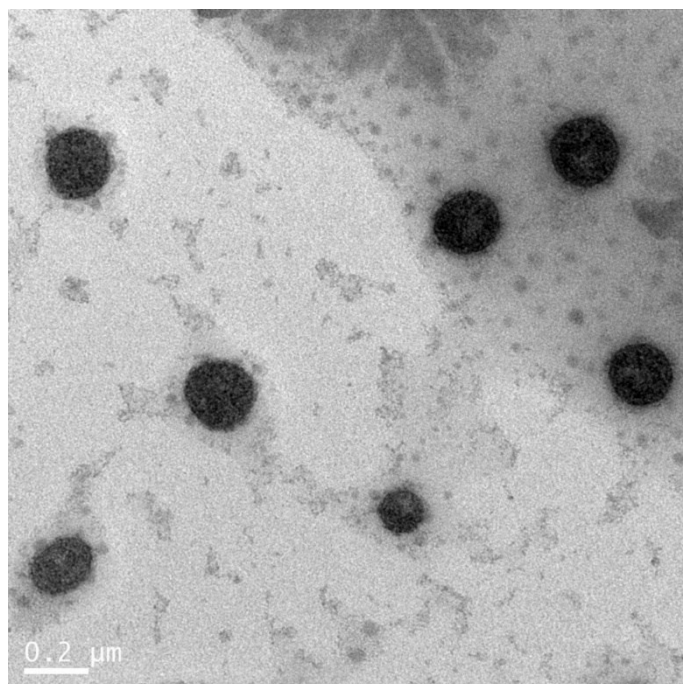


Fig. S18 TEM image of **FBC-200**.

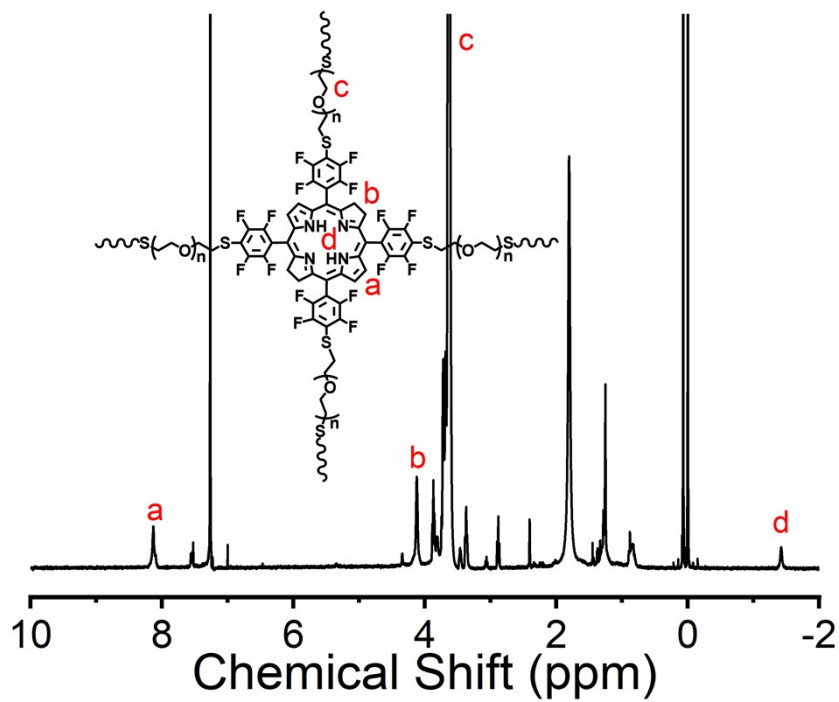


Fig. S19 ^1H NMR spectrum of FBC-80.

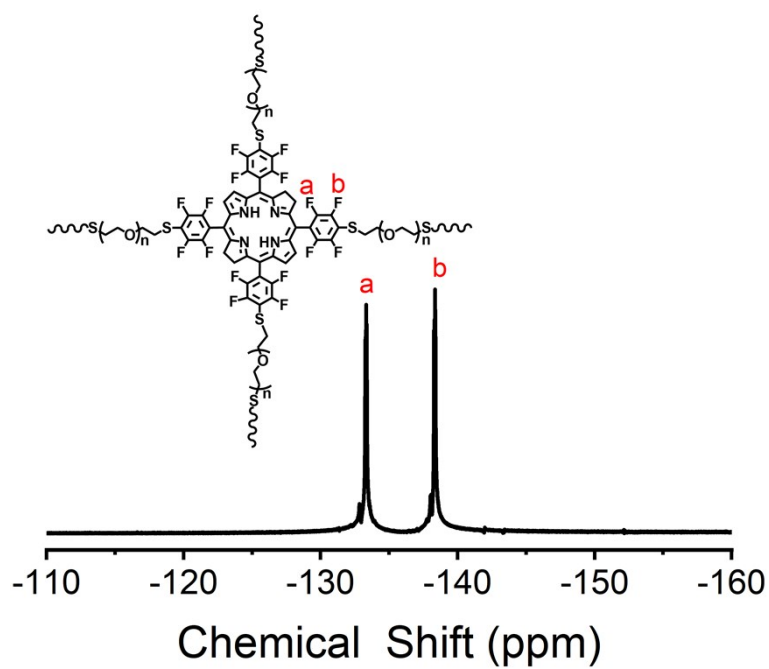


Fig. S20 ^{19}F NMR spectrum of FBC-80.

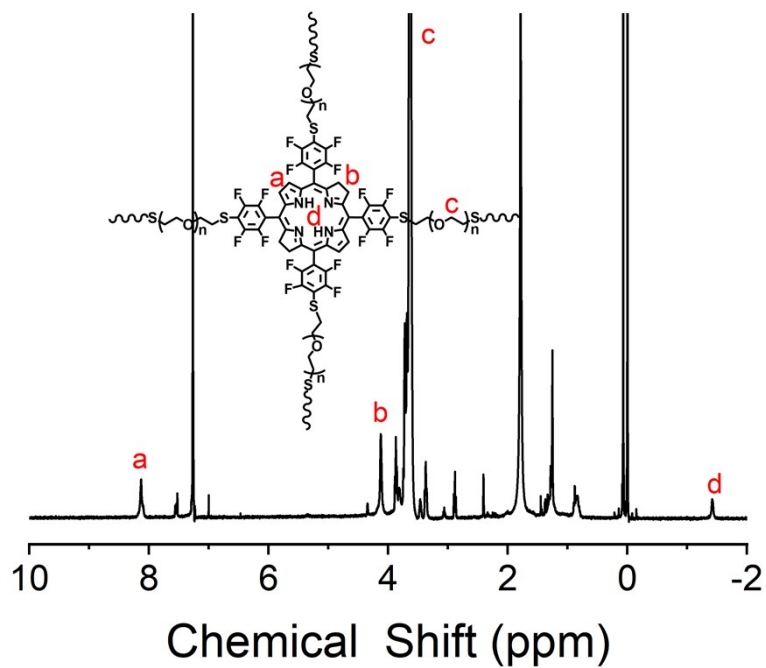


Fig. S21 ¹H NMR spectrum of FBC-200.

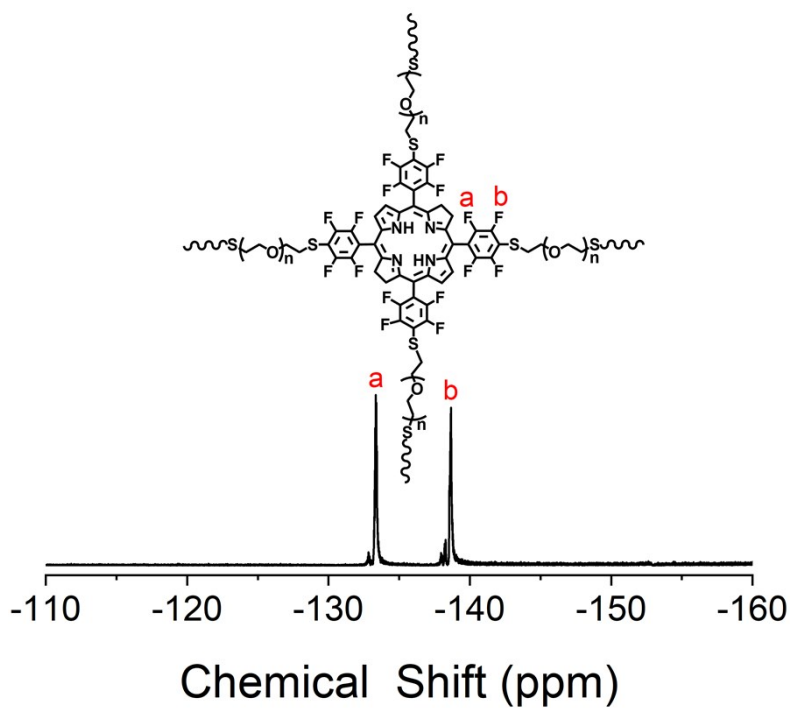


Fig. S22 ¹⁹F NMR spectrum of FBC-200.

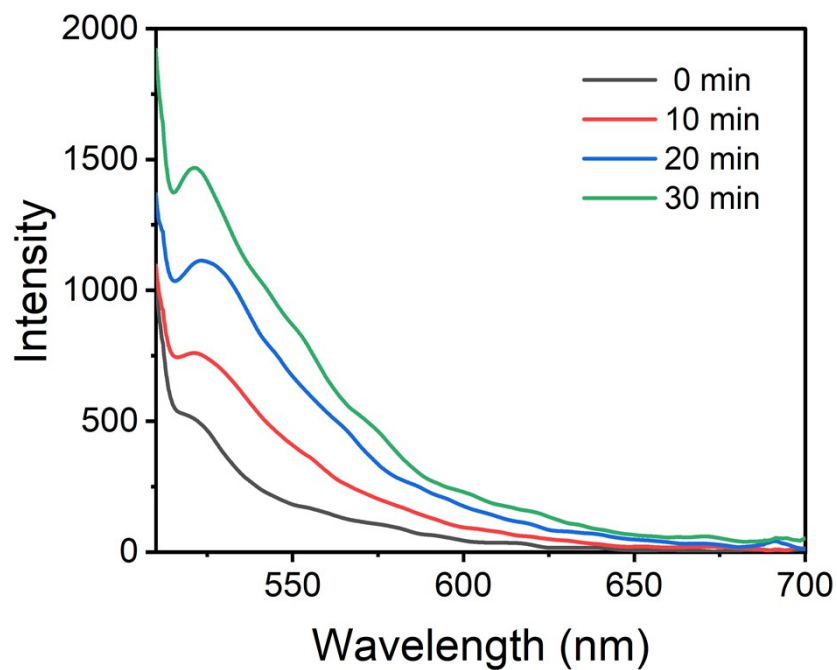


Fig. S23 Fluorescence spectra of HPF for $\cdot\text{OH}$ detection of **FBC** nanogels with increasing illumination time.

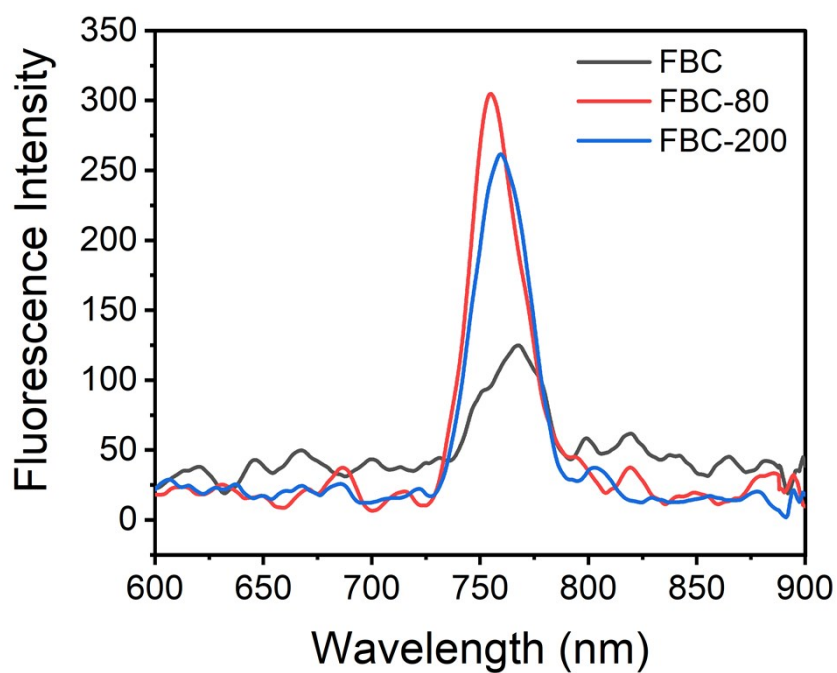


Fig. S24 The fluorescence Intensity of **FBC**, **FBC-80** and **FBC-200**.

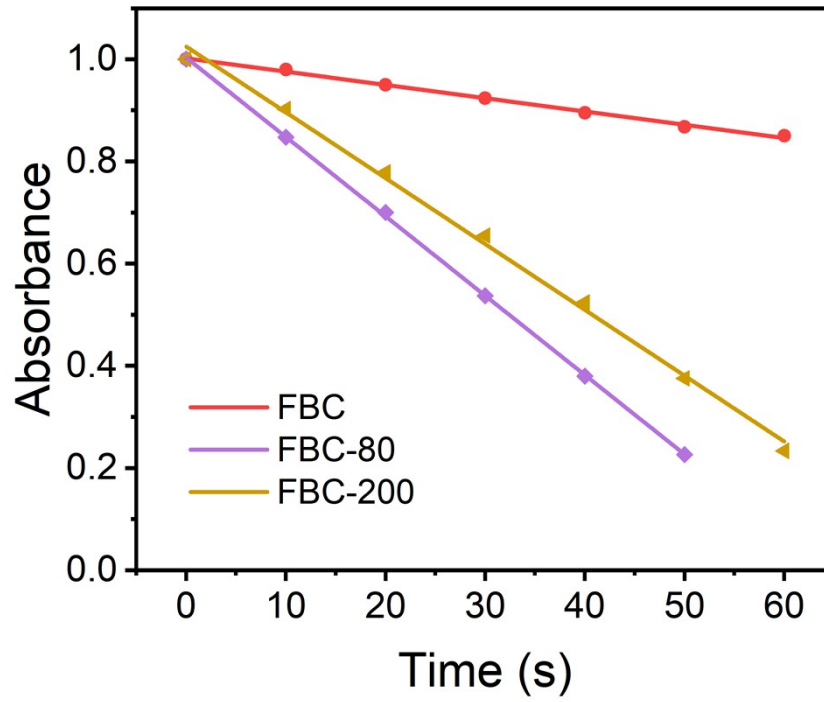


Fig. S25 ROS generation determined by DPBF.

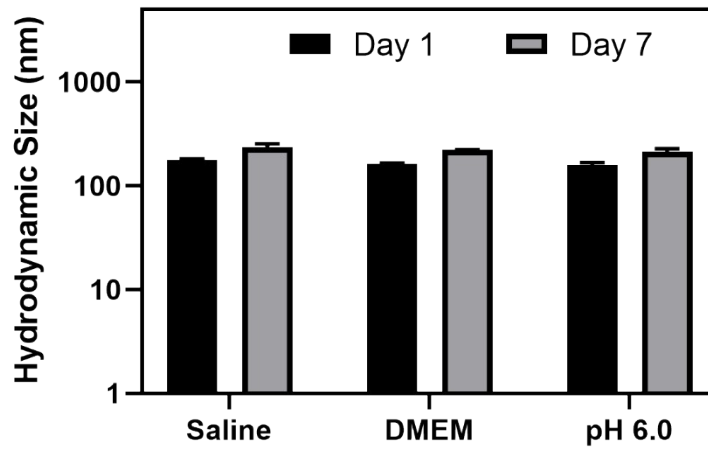


Fig. S26 Hydrodynamic size of FBC-200 under different conditions.

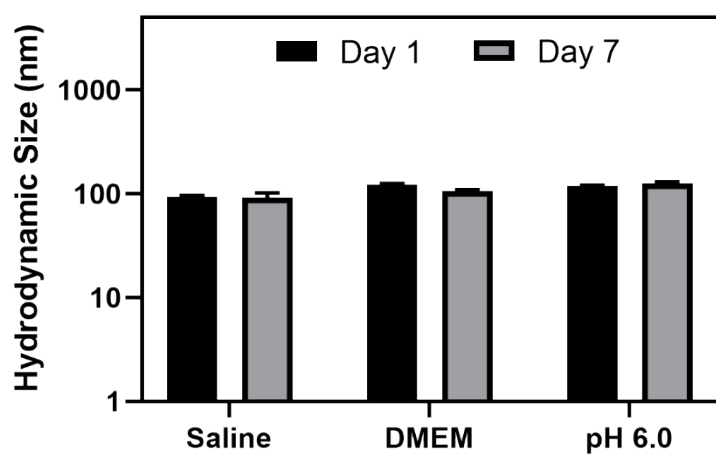


Fig. S27 Hydrodynamic size of FBC-80 under different conditions.

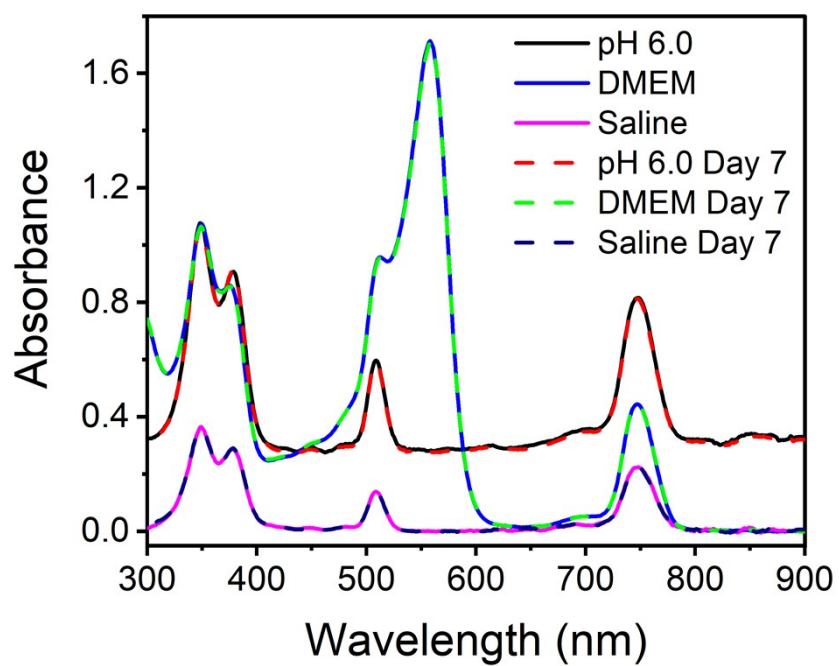


Fig. S28 UV-Vis spectra of FBC-200 under different conditions.

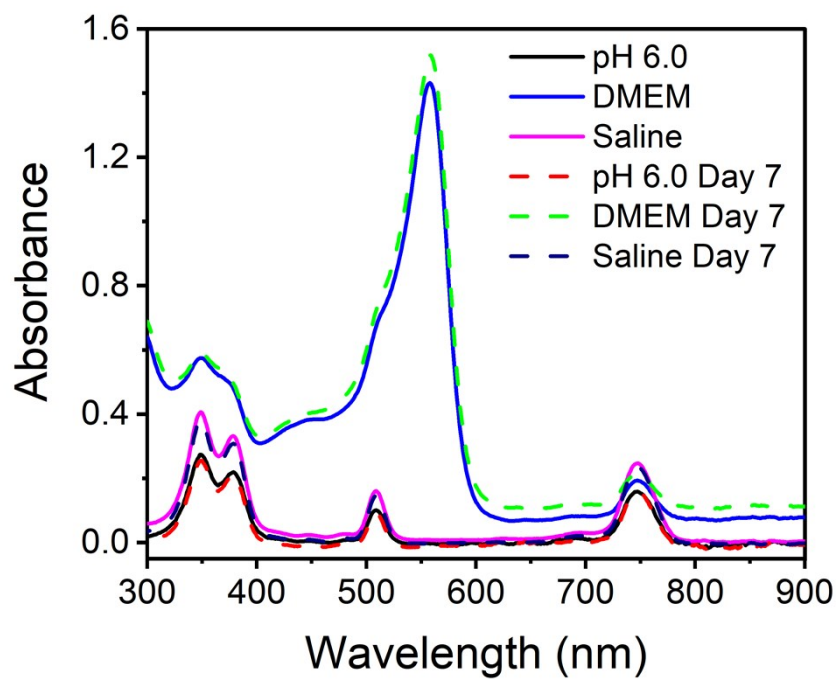


Fig. S29 UV-Vis spectra of **FBC-80** under different conditions.

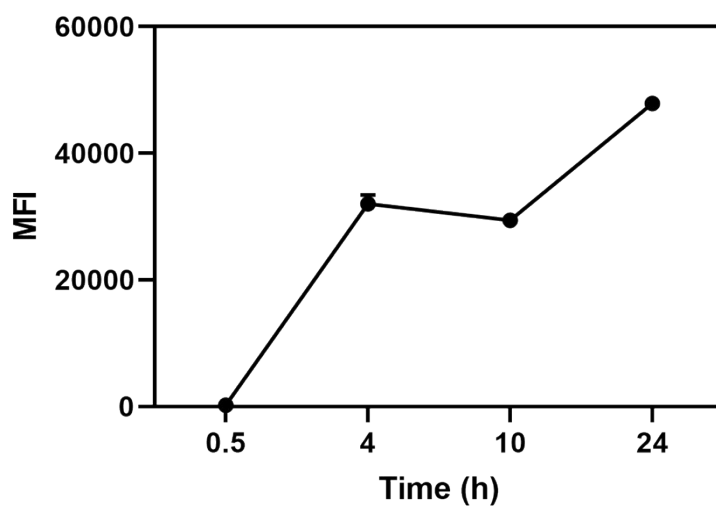


Fig. S30 Quantitative fluorescence intensity of tumors after intravenous injection of **FBC-200**.

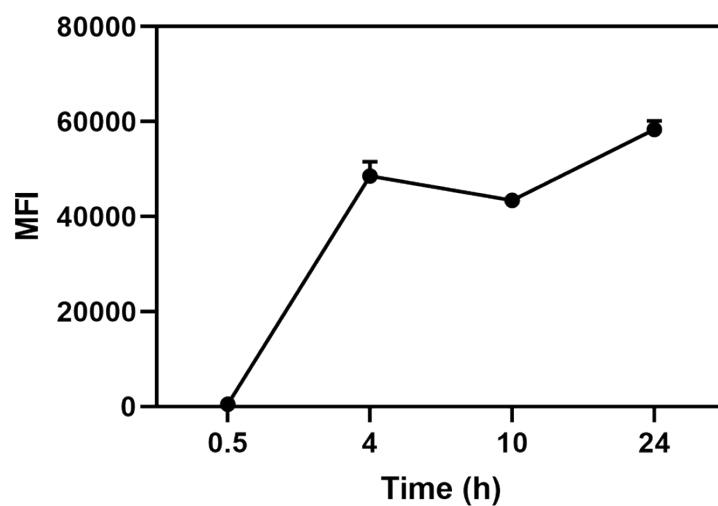


Fig. S31 Quantitative fluorescence intensity of tumors after intravenous injection of FBC-80.

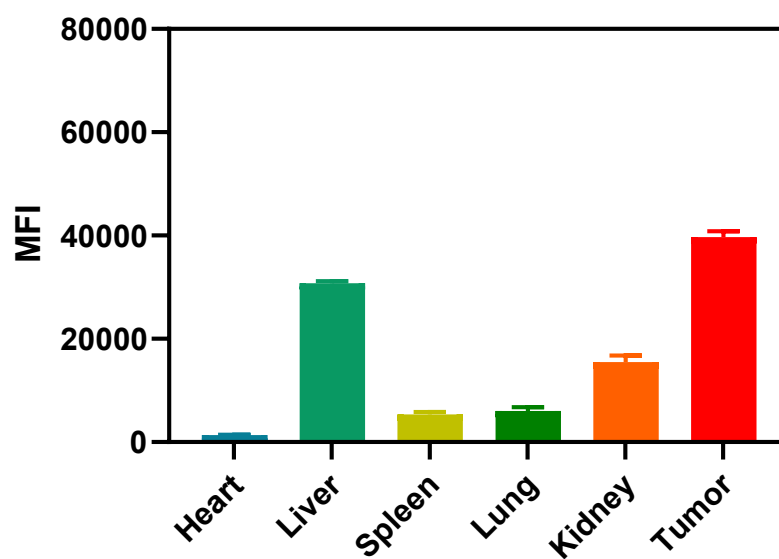


Fig. S32 Biodistribution of FBC-200 at 24 h.

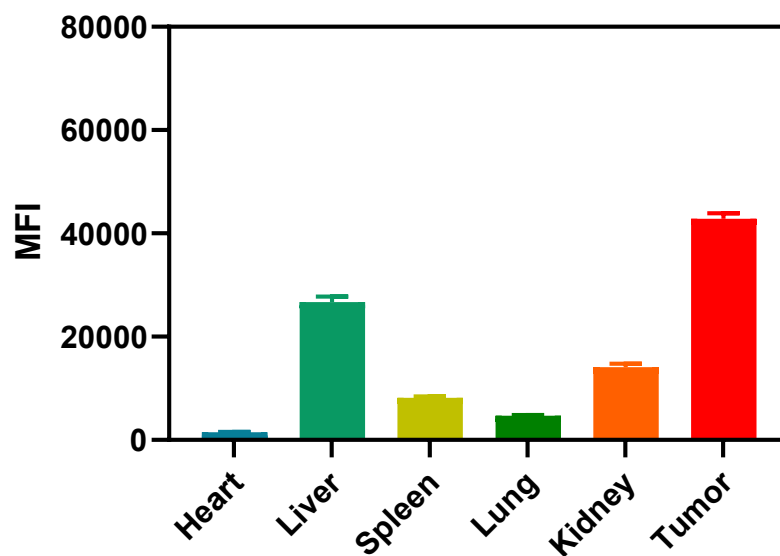


Fig. S33 Biodistribution of FBC-80 at 24 h.

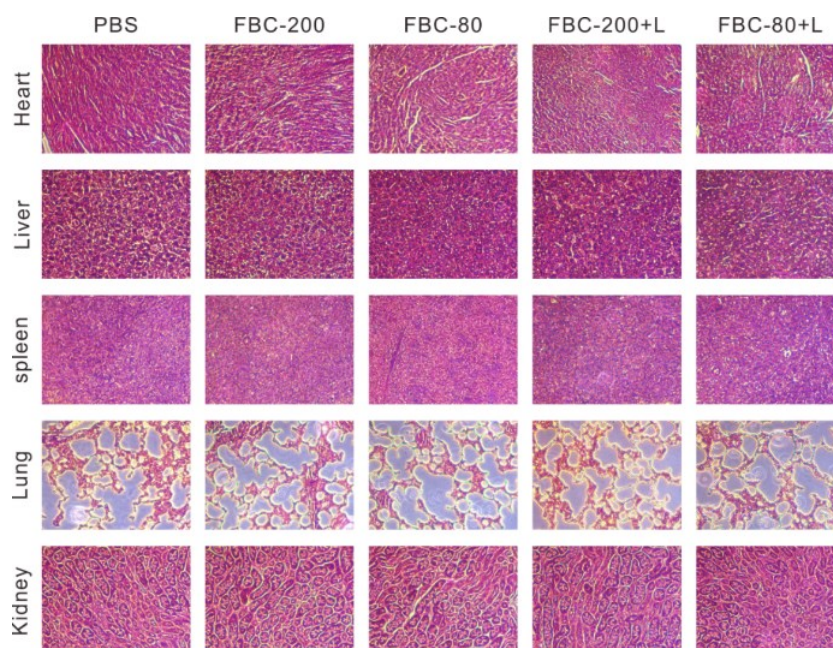


Fig. S34 H&E stained images of major organs from mice with different treatments.